The functions of ocu-miR-205 in regulating hair follicle development in Rex rabbits

Gongyan Liu
Shandong Agricultural University
Shu Li
Shandong Agricultural University
Hongli Liu
Shandong Agricultural University
Yanli Zhu
Shandong Agricultural University
Liya Bai
Shandong Academy of Agricultural Sciences
Haitao Sun
Shandong Academy of Agricultural Sciences
Shuxia Gao
Shandong Academy of Agricultural Sciences
Wenxue Jiang
Shandong Academy of Agricultural Sciences
Fuchang Li (chlf@sdau.edu.cn)
Shandong Agricultural University https://orcid.org/0000-0002-5670-8038

Research article

Keywords: ocu-miR-205, Dermal papilla cell, Rex rabbit, Hair follicle density

Posted Date: March 30th, 2020

DOI: https://doi.org/10.21203/rs.2.13789/v3

Version of Record: A version of this preprint was published at BMC Developmental Biology on April 22nd, 2020. See the published version at https://doi.org/10.1186/s12861-020-00213-5.

Abstract

Background: Hair follicles is an appendage from the vertebrate skin epithelium, and arise from the embryonic ectoderm andregenerate cyclically during adult life. Dermal papilla cells (DPCs) is the key dermal component of the hair follicle that directly regulates hair follicle development, growth and regeneration. Recent studies have reported that miRNA plays an important role in regulating hair follicle morphogenesis, proliferation, differentiation and apoptosis of hair follicle stem cells.

Results: The miRNAs expression profile of the DPCs from different hair density Rex rabbits shown that 240 differentially expressed of miRNAs were screened (log 2 (HD/LD)>1.00 and Q-value≤0.001). Among them, the expression of ocu-miR-205-5p in low hair densities DPCs was higher than that in high hair densities, and it is highly expressed in the skin tissue of Rex rabbits (P <0.05). ocu-miR-205 could increase cell proliferation and cell apoptosis ratio, change cell cycle process (P <0.05), affect the genes expression of PI3K/Akt, Wnt, Notch and BMP signaling pathways in DPCs and skin tissue of Rex rabbits, inhibit the protein phosphorylation level of CTNNB1, GSK-3β and the protein expression level of noggin (NOG), promote Akt phosphorylation level (P <0.05). There was no significant change in primary follicle density (P >0.05), but the secondary follicle density and total follicle density (P <0.05) were changed after ocu-miR-205-5p interfered expression, and secondary/primary ratio (S/P) in ocu-miR-205-5p interfered expression group increased at 14 days after injection (P <0.05).

Conclusion: ocu-miR-205 could promote the apoptosis of DPCs, affect PI3K/Akt, Wnt, Notch and BMP signaling pathways genes and proteins expression in DPCs and skin of Rex rabbits, promote the transformation of hair follicles from growth phase to regression and resting phase, and affect hair density of Rex rabbits.

Background

Rex rabbits are typically used for fur production because their fur is short, fine, dense, and smooth and has important economic value [1]. The most important indicator for evaluating the quality of Rex rabbit fur is the density of hair follicles [2]. In recent years, methods to improve the hair follicle density of Rex rabbits have become the most important concern in rabbit production. Hair follicles are an appendage from the vertebrate epithelium in the skin, arise from the embryonic ectoderm, and regenerate cyclically during adulthood [3]. The process of hair follicle formation and differentiation involves at least 20 different cells and tissues [4], including the dermal papilla, hair matrix, inner root sheath, and outer root sheath, as well as different signalling pathways, such as the Wnt, Notch, bone morphogenetic protein (BMP), and fibroblast growth factor (FGF) pathways, among others [5-9]. Phosphatidylinositol 3'-kinase (PI3K) preferentially phosphorylates PIP2 to produce PIP3, and PIP3 is an important second messenger in cells that subsequently activates Akt, and thus it plays an important role in regulating the proliferation and apoptosis of hair follicle cells. The Wnt signalling pathway regulates epithelial morphogenesis, hair follicle development and cell differentiation. The PI3K/Akt signalling pathway inhibits the phosphorylation of β-catenin by phosphorylating glycogen synthase kinase 3β (GSK-3β) and activates the Wnt signalling pathway[5]. Dickkopf-related protein 1 (DKK1) inhibits the Wnt signalling pathway by inhibiting the phosphorylation of β-catenin and induces hair follicle regression [10]. When Notch receptor binds to a ligand, it activates hair follicle stem cells and then promotes the transition of hair follicles from the resting stage to growing stage[6]. The BMP signalling pathway is involved in embryonic skin appendage organ morphogenesis and postnatal hair follicle growth[7]. The BMP2 and BMP4 genes inhibit hair follicle development and are associated with maintaining hair follicles in the resting stage[8]. Noggin (NOG) is an inhibitor of the BMP signalling pathway, and its abnormal expression leads to follicular enlargement [7]. The Notch signalling pathway interacts with the BMP signalling pathway, and the BMP signalling pathway inhibits the Wnt signalling pathway by regulating β-catenin expression [6]. Dermal papilla cells (DPC) is a population of mesenchymal cells aggregated in hair bulbs and the key dermal component of the hair follicle, it can directly regulate hair follicle development, growth and regeneration [11]. Moreover, the number of DPCs also specifies the hair size, shape and cycling [12]. Signal exchange between DPCs and hair follicle stem cells at telophase is the key to initiating the next hair follicle cycle [13].

MicroRNAs (miRNAs) are small non-coding RNAs that have been proposed to play important roles in organ development, cell proliferation, tumourigenesis, lipid metabolism, behaviour, embryogenesis and other biological processes [14-19]. Recently,

miRNAs were reported to play important roles in regulating hair follicle morphogenesis and the proliferation, differentiation and apoptosis of hair follicle stem cells in mice, rats, goats and sheep [20-22]. Notably, miR-214 inhibits hair follicle growth and development by modulating the expression of regulatory factors in Wnt signalling pathway, such as β-catenin and lymphoid enhancer-binding factor 1 (Lef-1) [23]. Upon the overexpression of DKK1 in transgenic mice, the expression of miR-200b and miR-196a in epidermis decreases significantly, which is possibly mediated by potential target genes acting on the Wnt signalling pathway [24]. As shown in a previous study, miR-let-7b promotes alpaca hair growth by inhibiting the transcription of transforming growth factor β receptor 1 (TGFβR1) [25]. BMP4 negatively regulates the expression of miR-21, and miR-21 negatively regulates the expression of the BMP-dependent tumour suppressor genes Pten, Pdcd4, Timp3 and Tpm1 [26]. Hair follicle development and hair growth in mice are regulated by miR-31 through effects on the BMP and Wnt signalling pathways [20]. Additionally, miR-205 is a highly conserved miRNA that shares a similar expression pattern with miR-200 family [27]. It is one of the miRNAs expressed at the highest levels in the epidermis [28, 29], and it plays an essential role in promoting the neonatal expansion of skin stem cells during early development by modulating the PI3K pathway [30].

We isolated the DPCs from the skin of Rex rabbits and analysed the miRNA expression profiles of the DPCs from Rex rabbits with different hair densities to improve the fur quality of Rex rabbits. Among the miRNAs analysed, ocu-miR-205 was one of the miRNAs expressed at the highest levels in DPCs. We examined the function of ocu-miR-205 in hair follicle development.

Results

DPCs show a complex miRNA expression pattern

We evaluated the varieties of miRNAs in DPCs from 30-day-old Rex rabbits with lower and higher hair densities (Additional file 1) by subjecting RNA samples with a high integrity and qualified quality (Additional file 2) to high-throughput small RNA sequencing using the BGISEQ-500 platform. We obtained 37930744, 39442011, 40965907, 38502653, 40622117 and 41149163 clean reads from the six samples (Additional file 3), and the majority of clean reads had a length of 23 nucleotides (Additional file 4), consistent with the size of mammalian miRNAs. After a comparison with known small RNA databases, more than 90 % of the clean reads in the six libraries were matched, and the percentage of matching reads for each library was 91.91 %, 91.05 %, 92.46 %, 92.77 %, 90.13 %, and 91.61 %, respectively (Additional file 5). The results of the small RNA classification showed that miRNAs accounted for 80.80 %, 82.50 %, 81.60 %, 85.80 %, 76.50 %, and 81.80 % of the small RNAs, respectively (Additional file 6). The base Q20 value of filtered data was greater than 90 % and the Q30 value was greater than 80 %, indicating that the quality of the data was reliable. Additional files 7 and 8 show the quantity and quality distribution maps of the bases in each sample, respectively.

By screening differentially expressed genes (DEGs), 240 differentially expressed miRNAs were identified ($\log_2$(HD/LD)>1.00 and Q-value≤0.001; Fig. 1a and Additional file 9), including 122 miRNAs that were upregulated and 118 miRNAs that were downregulated (Fig. 1b). The annotation of the target genes of differentially expressed miRNAs was performed using Gene Ontology (GO) enrichment and Kyoto Encyclopaedia of Genes and Genomes (KEGG) pathway analysis. A total of 205,661 target genes were enriched in GO terms (Fig. 1c). Specific GO terms of the target genes mainly involved in the biological process (BP), cellular component (CC) and molecular function (MF) categories. Following the GO analysis, the target genes were also uploaded into the KEGG database to identify the pathways that were actively regulated by miRNAs in DPCs. Three hundred twenty-five pathways were predicted. The top enriched pathways were the Wnt signalling pathway and Notch signalling pathway, among others (Fig. 1d).

The expression of ocu-miR-205

The structure of one of the differentially expressed miRNAs, ocu-miR-205, is shown in Fig. 2a. The expression of ocu-miR-205 differed in DPCs from Rex rabbits with different hair densities ($\log_2$(HD/LD)>1.00 and Q-value≤0.001; Fig. 2b) and was expressed at low levels in DPCs from Rex rabbits with a high hair density (HD) and at high levels in DPCs from Rex rabbits with a low hair density (LD). Quantitative fluorescence PCR results also confirmed the accuracy of the ocu-miR-205-5p

sequencing results (Fig. 2c). Furthermore, the expression of ocu-miR-205-5p in different tissues from Rex rabbits differed (P<0.05). The expression in the skin tissue was higher than in the stomach, intestine, spleen, liver, heart, lung, kidney, muscle and fat (P<0.05; Fig. 2d), suggesting a tissue-specific expression pattern.

Effects of ocu-miR-205 on DPCs from Rex rabbits

HBAD-GFP, HBAD-ocu-miR-205-GFP, and HBAD-ocu-miR-205-5p-sponge-GFP were constructed and used to transfect DPCs at a multiplicity of infection (MOI) of 200. Cell proliferation, the cell cycle, cell apoptosis, and changes in the expression of ocu-miR-205-5p and hair follicle development-related genes and proteins were detected 48 h after transfection. The constructed adenoviruses successfully transfected DPCs (Fig. 3a), and ocu-miR-205-5p expression increased significantly after overexpression, but decreased significantly after silencing (P<0.05; Fig. 3b). Importantly, ocu-miR-205 increased cell proliferation and the cell apoptosis rate, in addition to altering the progression of the cell cycle (P<0.05; Table 1). Moreover, ocu-miR-205 inhibited the expression of the Inppl1, Frk and Phlda3 mRNAs, which are involved in the PI3K/Akt signalling pathway (P<0.05). The expression of ocu-miR-205 induced the expression of the DKK1 mRNA and inhibited the expression of the Wnt10b, CTNNB1 and GSK-3β genes in the Wnt signalling pathway (P<0.05). The expression of the Notch1, Jagged1, Hes1 and Hes5 genes in the Notch signalling pathway was suppressed by ocu-miR-205 (P<0.05), whereas the expression of the BMP2, BMP4 and TGF-β1 genes in the BMP signalling pathway was induced (P<0.05; Table 2). The expression of ocu-miR-205 inhibited the phosphorylation of the CTNNB1 and GSK-3β proteins, decreased the level of the noggin (NOG) protein, and increased the level of Akt phosphorylation (P<0.05; Fig. 4).

Effects of ocu-miR-205 on the skin tissue of Rex rabbits

One hundred 3-month-old Rex rabbits with similar body weights were randomly divided into 4 groups. After local shaving of the back skin, 50 μL of HBAD-GFP, HBAD-ocu-miR-205-GFP and ocu-miR-205-5p-sponge-GFP were injected intradermally into the rabbits in each group. 24 h after the injected, one randomly selected Rex rabbit from each group was euthanized, and frozen sections were prepared from the locally injected skin to confirm the expression of the miRNAs from the injected adenoviruses. Eight Rex rabbits were randomly selected from each group 7 days, 14 days and 21 days after transfection. After euthanasia, the injected skin was collected and divided into two parts. A part placed in freezing tube and the other part was fixed at a 4 % paraformaldehyde fixative solution. The frozen samples were used to detect the changes in the expression of ocu-miR-205-5p and hair follicle development-related genes and proteins. The fixed samples were used to prepare paraffin sections, and the hair density was counted after HE staining. The constructed adenoviruses successfully transfected the skin and hair follicles of Rex rabbits (Fig. 5a), and the expression of ocu-miR-205-5p increased significantly after overexpression, but decreased significantly after silencing (P<0.05; Fig. 5b). Fourteen days after the injection, ocu-miR-205 significantly altered the expression of genes involved in the PI3K/Akt, Wnt, Notch and BMP signalling pathways (P<0.05; Table 3). Moreover, ocu-miR-205 significantly altered the levels of the phosphorylated CTNNB1, GSK-3β, and Akt proteins and the level of the NOG protein (P<0.05; Fig. 6). A significant change in the primary follicle density was not observed (P>0.05), but the secondary follicle density and total follicle density (P<0.05) were altered after ocu-miR-205-5p interfered expression, and the secondary/primary ratio (S/P) in the ocu-miR-205-5p interfered expression group increased at 14 days after the injection (P<0.05; Table 4).

Discussion

Rex rabbits are typically used for fur production, and the skin quality is the most important factor. The hair follicle cycle can typically be divided into anagen, catagen, and telogen phases[31]. Similar to the Cashmere goat, the Rex rabbit has a double-coat skin, which contains primary and secondary hair follicles[32]. The hair follicles postnatally enter into the cycle. The hair follicle growth cycle and obviously different sizes of primary and secondary hair follicles enable the easy differentiation of hair cycle phases and hair follicle types [33]. Many factors affect the growth and development of hair follicles in Rex rabbits, such as genetic, nutritional, age, among others [34-37]. The most hair follicles in anagen phases when the Rex rabbits at 4-5 weeks[37]. Notably, miRNAs are considered key regulators of gene expression at the post-transcriptional level and perform a

variety of important functions within cells, such as the regulation of growth, metabolism, development and cell differentiation [38-40]. Among them, miR-205 is a keratinocyte-specific miRNA that is abundantly expressed in the epidermis [41, 42]. It has an essential role in promoting the neonatal expansion of skin stem cells during early development by modulating the PI3K/Akt signalling pathway [43]. Although the effects of miR-205 on keratinocyte migration have been investigated in some in vitro models [44, 45], in vitro studies using both primary human epidermal keratinocytes and corneal epithelial keratinocytes indicate that miR-205 promotes keratinocyte migration by targeting the lipid phosphatase SHIP2 and KIR4.1, respectively [44, 45]. DPCs of various origins induce the de novo formation of the hair follicle structure in both follicular and afollicular epidermis [46-49], implying a potential therapeutic application of DPCs in the treatment of alopecia. In the present study, ocu-miR-205-5p was expressed at significantly higher levels in DPCs from rabbits with low hair densities than in DPCs from rabbits with high hair densities. Moreover, ocu-miR-205 induced G0/G1 arrest in DPCs, which was further confirmed by the reduction in the population of DPCs in the G0/G1 phase and increase in the apoptotic rate after the transfection of the ocu-miR-205 inhibitor. This finding is consistent with previous studies [50]. Furthermore, overexpression of miR-205 significantly inhibited cell proliferation. Additionally, ocu-miR-205 inhibited the expression of related gene and proteins in the PI3K/Akt, Wnt, and Notch signalling pathways, and activated the BMP signalling pathway. Therefore, ocu-miR-205 plays an important role in regulating hair follicle development.

Conclusions

In conclusion, ocu-miR-205 promoted the apoptosis of DPCs, inhibited cell proliferation, modulated the expression of genes and proteins involved in the PI3K/Akt, Wnt, Notch and BMP signalling pathways in DPCs and the skin of Rex rabbits, promoted the transition of hair follicles from the growth phase to the regression and resting phase, and altered the hair density of Rex rabbits.

Methods

Animal and sample collection

The Rex rabbits used in this study were purchased from Taishan Rabbit Farm (Shandong, China). Ten adult female Rex rabbits with a high (>14000/cm^2) or low hair density (<10000/cm^2) were chosen and divided into 2 groups. An adult male rabbit was selected to mate with the female rabbits within each group. The first generation of offspring (F1 generation) was obtained and then inbred with F1 in the same nest (high density and high density, low density and low density inbreeding). Three rabbits each with high and low hair densities were selected from the second generation of offspring (F2 generation) 30 days after birth. Selected animals were electrically stunned (120 V, pulsed direct current, 50 Hz for 5 s) and euthanized by exsanguination of the carotid artery and before skin was harvested from the experimental rabbits. The DPCs were separated and cultured, methods according to references[51,52]. After the cells had established a monolayer (approximately 12 days), the total RNA was extracted, tested for quality.

Construction of the small RNA libraries, sequencing analysis, miRNA identification and prediction of new miRNAs in DPCs

Small RNA fragments measuring 18–30 nt were isolated and purified from the total RNA using 15 % denaturing polyacrylamide gel electrophoresis (PAGE). Subsequently, 3' and 5' RNA adaptors were ligated to the RNA pool using T4 RNA ligase, and the samples were used as templates for cDNA synthesis. The cDNAs were amplified using the appropriate number of PCR cycles needed to produce the sequencing libraries, which were subsequently subjected to the proprietary Solexa sequencing by synthesis method using the BGISEQ-500 platform at Shenzhen Huada Biotech Co., Ltd. [53, 54] (Shenzhen, China).

The raw reads produced from BGISEQ-500 sequencing were filtered to remove low-quality reads, and reads that passed the quality filter were trimmed to remove the 5' and 3' adaptor sequences. Similarly, the reads with a poly (A) sequences were excluded. The length distribution of the clean reads was calculated. The remaining reads were analysed using BLAST with

Bowtie-1.0.0 software, Rfam [55] and Repbase to discard messenger RNA (mRNA), ribosomal RNA (rRNA), transfer RNA (tRNA), small nuclear ribonucleic acid (snRNA), small nucleolar RNA (snoRNA) and repeat sequences. The remaining sequences were used for miRNA identification and compared with the mature miRNAs and pre-miRNAs from *Oryctolagus cuniculus* listed in miRBase 21.0 [56], with permission of one mismatch. Subsequently, the miRDeep 2 software [57] was used to predict the novel miRNAs by exploring the secondary structure, Dicer cleavage sites and minimum free energy of the unannotated small RNA tags that mapped to the *Oryctolagus cuniculus* genome. The sequences remaining after the identification of conserved miRNAs were aligned to the *Oryctolagus cuniculus* genome to identify new *Oryctolagus cuniculus* miRNAs. Certain target sequences around the small RNAs were used to explore the secondary structures and folding energy (218 kcal/mol).

Transcripts per million (TPMs) were calculated to standardize the expression levels of small RNA [58], which potentially avoided the effect of different sequencing quantities on quantitative accuracy. Based on the assumption that RNA sequencing is a random process, namely, each sequence is uniformly randomly amplified from its own sample [59], the expression of each transcript is presumed to exhibit a binomial distribution. Using the model described above, DEGseq calculated differential expression based on MA-plot [60, 61]. Assuming that C1 and C2 are the total reads in the comparison of two samples, they exhibit a binomial distribution, where Textit {M}= $\log_2$ C1 - $\log_2$ C2, A= ($\log_2$ C1 + $\log_2$ C2)/2. Under the condition of random sampling, the distribution of M obeys A=a and approximates a normal distribution. The P-value of each miRNA was corrected by performing multiple hypothesis tests using Q-values. When the difference in coincidence was more than two-fold and the Q-value was less than or equal to 0.001, the miRNAs were considered significantly differentially expressed.

The miRNAs were aligned to the EST unigenes of *Oryctolagus cuniculus* and the target genes were predicted using the miRanda algorithm to obtain a better understanding of the potential functions of the significantly differentially expressed miRNAs in Rex rabbits with different hair densities [62]. An enrichment analysis of the predicted target genes was conducted with GO terms and KEGG pathways [63].

Construction and identification of adenovirus vectors overexpressing and silencing ocu-miR-205

HBAD-GFP (HANBIO adenovirus-green fluorescent protein; empty vector), HBAD-ocu-miR-205-GFP (overexpression), HBAD-ocu-miR-205-5p-sponge-GFP (silencing) adenoviruses were synthesized and constructed by Hanheng Biotechnology Co., Ltd. (Shanghai, China). The infective titres of HBAD-GFP, HBAD-ocu-miR-205-GFP and HBAD-ocu-miR-205-5p-sponge-GFP were $1.26*10^{10}$ PFU/mL, $1.58*10^{10}$ PFU/mL and $1.26*10^{10}$ PFU/mL, respectively.

Third-generation DPCs displaying good growth conditions were inoculated into a disposable 6-well plate. The cell density was approximately $1.0*10^5$ cells/mL. Prior to the infection, the virus was subjected to 10-fold gradient dilution. Generally, the MOI (multiplicity of infection) was controlled in the range of 10-1000. HBAD-GFP, HBAD-ocu-miR-205-GFP and HBAD-ocu-miR-205-GFP were individually transfected into Rex rabbit DPCs at an MOI 200, and a negative control was established using cells undergoing normal culture.

Fifty microliters of the purified adenovirus were injected into the skin of each Rex rabbit with microinjector at a concentration of $5.0*10^8$ - $1.0 * 10^9$ virus particles per Rex rabbit after shaving the middle part of the back of 100 3-month-old Rex rabbits with similar body weights and good health. Twenty-four h after transfection, one Rex rabbit from each group was randomly selected, euthanized, and frozen sections were prepared from the locally injected skin. The adenovirus-transfected skin was observed under a positive fluorescence microscope (Nikon ECLIPSE 80i, Japan).

Assessment of the proliferation, cell cycle and apoptosis of DPCs

DPCs were plated in a 96-well plate at a density of 10^4 cells/well, cultured in basal medium for 24 h, and then transfected with the indicated adenoviruses. Twenty microliters of a 5 g/L thiazolyl blue tetrazolium bromide (MTT) solution (Solarbio, Beijing, China) were added to each well and incubated for 4 h. Next, dimethyl sulfoxide (DMSO, Solarbio, Beijing, China) was

added to each well and incubated at 37 °C. Optical density (OD) values were recorded at 490 nm using an enzyme labelling instrument (BioTek Elx-808, USA) after 10 min of oscillation. Within a certain cell number range, the amount of MTT crystallization is proportional to the number of cells. Using to the measured OD value, we calculated the number of living cells. A larger OD value indicates higher cell proliferation activity. For the flow cytometry analysis, DPCs were transfected with the indicated adenovirus. The cells were digested with trypsin and fixed with 70 % cold ethanol for at least 18 h. Cells were then centrifuged at 500 g for 5 min, the supernatant was discarded, and added 0.5 mL of propidium iodide (PI; BD Biosciences, Cat: 550825) was incubated with the cells for 15 min at 37 °C in the dark. The cells were then analysed using flow cytometry (BD Accuri C6, BD). The results were analysed with the ModFit LT 5.0 software.

Third-generation DPCs were plated in a disposable 6-well plate at a density of 10^4 cells/mL, with 2 mL of the cell suspension plated in each well. After a 24-h incubation to allow cells to adhere, the culture medium was removed. After treatment and culture for a certain time, the cells were digested with a trypsin digestion solution lacking EDTA (Solarbio, Beijing, China). Cells were centrifuged and collected into a 1.5 mL centrifugal tube, and then washed with PBS. After centrifugation, 500 μL of 10X Annexin V Binding Buffer was added to re-suspended the cells, followed by the labelling of F-actin. Cells were incubated with the FITC Annexin V and Propidium Iodide Staining Solution for 15 min at 4 °C and then analysed using flow cytometry. The percentages of early apoptotic cells (Q4), late apoptotic cells (Q2) and total apoptotic cells (Q2 + Q4) in each sample were calculated.

Total RNA extraction and Real-time PCR analysis

Total RNA was extracted from tissues or cells with the RNAiso reagent (TaKaRa, Japan), according to the manufacturer's instructions. The integrity and quality of the total RNA were evaluated using a 2100 Bioanalyzer RNA Nano chip device (Agilent, Santa Clara, CA, USA) and agarose gel electrophoresis, respectively, and the concentration was measured with an ND-1000 spectrophotometer (NanoDrop, Wilmington, DE).

For quantitative RT-PCR of mRNA, 1 μg of total RNA of was used to synthesize cDNAs with a Transcriptor First Strand cDNA Synthesis Kit (Roche Diagnostics GmbH Mannheim, Germany). Quantitative RT-PCR was performed to determine the expression levels of target mRNAs, and glyceraldehyde-3-phosphate dehydrogenase (GAPDH) served as the reference gene. All quantitative PCR primers (Additional file 10) were designed using Primer Premier 5 software and synthesised by SANGON Biological Engineering Co., Ltd. (Shanghai, China). PCR amplification was performed using the Fast Start Universal SYBR Green Master Mix (Roche Diagnostics GmbH Mannheim, Germany). The volume of each reaction was 20 μL, including 2 μL of cDNAs, 10 μL of SYBR Premix Ex Taq^{TM} (2×), 0.5 μL of the PCR Forward Primer (10 μM), 0.5 μL of the PCR Reverse Primer (10 μM), 0.4 μL of ROX Reference Dye II (50×) and 6.6 μL of ddH_2O. The number of cycles set for the linear amplification of the cDNAs was 40. All samples were analysed in duplicate, and the standard curves were generated using pooled cDNAs from the samples being assayed.

For the quantitative RT-PCR of miRNAs, 1 μg of total RNA was reverse transcribed with Bulge-Loop miRNA-specific reverse transcription primers (RiboBio, China), and quantitative PCR was performed using Fast Start Universal SYBR Green Master Mix (Roche Diagnostics GmbH Mannheim, Germany) and Bulge-Loop primers (RiboBio, Guangzhou, China) on the 7500 Fast System 1.4 system with small nuclear RNA U6 as the normalisation control. The volume of each reaction was 20 μL, including 2 μL of cDNAs, 10 μL of SYBR Green Master (2X), 0.8 μL of the Bulge-Loop^{TM} miRNA Forward Primer (5 μM), 0.8 μL of the Bulge-Loop^{TM} Reverse Primer (5 μM), 0.4 μL of ROX Reference Dye II (50×) and 6.0 μL of ddH_2O. PCR was performed under the following conditions: 10 min of template denaturation at 95 °C, followed by 40 cycles of 95 °C for 2 s, 60 °C for 20 s, and 70 °C for 10 s. Melting curves (70 °C-95 °C) for each sample were analysed after each run to confirm the specificity of amplification reactions. Three biological replicates with three technical replicates were conducted for each qRT-PCR. The relative expression levels of mRNAs and miRNAs were calculated using the arithmetic formula $2^{-\triangle\triangle Ct}$ [65].

Western immunoblotting.

Tissues or cells were lysed in RIPA buffer on ice for 30 min. The supernatant was centrifuged at 12,000 g for 30 min at 4 °C, and protein concentrations were determined using a BCA Protein Assay Kit (Kangwei, China). The extracted proteins (50 ng/sample) were solubilized in 40 millimoles of SDS-loading buffer (Solarbio, China) and then resolved by electrophoresis (Bio-Rad, Richmond, USA) on 12.5 % SDS-PAGE gels prior to being electrophoretic transfer to polyvinylidene fluoride (PVDF) membranes (Millipore, Billerica, USA). The standard markers for protein molecular masses were purchased from Thermo (USA). The membranes were blocked with 5 % skimmed milk in PBS (Solarbio, China) at 4 °C overnight and incubated with primary antibodies (tubulin AT819, Beyotime, China; phospho-CTNNB1-S552 pAb, Abcam, US; phospho-GSK3B-S9 pAb, Abcam, US; phospho-AKT1-S473 pAb, Abcam, US; or NOG polyclonal antibody, Abcam, US). The membranes were then rinsed with Tris-buffered saline containing Tween (TBST; Solarbio, China), and subjected to detection with a 1:3000 dilution of a horseradish peroxidase (HRP)-conjugated goat anti-mouse IgG antibody (Beyotime, China) at 37 °C for 1 h. Proteins were visualized using BeyoECL reagents (Beyotime, China). The intensity of the bands was quantified with a Pro Plus 6.0 Biological Image Analysis System. The levels of phospho-CTNNB1, phospho-GSK3B, phospho-AKT1 and NOG were normalized to the internal control beta-tubulin, and the relative expression levels were calculated.

Statistical analysis

All data were analysed with SAS software (SAS version 8e; SAS Institute, Cary, NC, USA). A one-way ANOVA was used to evaluate the differences in mean values among various groups. The data are presented as the means and R-MSE. $P < 0.05$ was regarded as statistically significant.

Abbreviations

BMP: bone morphogenetic protein; BP: biological process; CC: cellular component; DAG: Directed Acyclic Graph; DEGs: differentially expressed genes; DMEM: Dulbecco's Modified Eagle's Medium; DMSO: dimethyl sulfoxide; DPCs: dermal papilla cells; DKK1: Dickkopf-related protein 1; FBS: foetal bovine serum; FGF: fibroblast growth factor; GAPDH: glyceraldehyde-3-phosphate dehydrogenase; GFP: green fluorescent protein; GO: Gene Ontology; GSK-3β: glycogen synthase kinase 3β; HD: high hair density; HE: haematoxylin and eosin; Lef-1: lymphoid enhancer-binding factor 1; LD: low hair density; miRNAs: microRNAs; mRNA: messenger RNA; MTT: thiazolyl blue tetrazolium bromide; NOG: noggin; rRNA: ribosomal RNA; S/P: secondary/primary ratio; snRNA: small nuclear ribonucleic acid; snoRNA: small nucleolar RNA; TGFβ: transforming growth factor β; TPM: transcripts per million; tRNA: transfer RNA; ocu-miR-205: *Oryctolagus cuniculus* microRNA 205; OD: optical density; PAGE: polyacrylamide gel electrophoresis; PBS: phosphate-buffered saline; PI3K: phosphatidylinositol 3'-kinase.

Declarations

Ethics approval and consent to participate

The experimental procedures were approved by the Committee of Ethics in Research of Shandong Agricultural University (SDAUA-2017-029) and performed in accordance with the Guidelines for Experimental Animals of the Ministry of Science and Technology (Beijing, China). This article does not any studies with human participants performed by any of the authors.

Consent for publication

Not applicable.

Availability of data and materials

The datasets used and/or analysed during the current study are available from the corresponding author on reasonable request.

Competing interests

The authors declare that they have no competing interests.

Funding

This study was supported by the Earmarked Fund for Modern Agro-industry Technology Research System (CARS-43-B-1), National Natural Science Foundation of China (31972594), and Funds of Shandong “Double Tops” Programme (SYL2017YSTD11). The funding bodies had no role in the design of the study and collection, analysis, and interpretation of data and in writing the manuscript.

Authors’ contributions

GL, SL and LB isolation, culture and identification of DPCs, and construction of the small RNA libraries, sequencing analysis, miRNAs identification and prediction of new miRNAs. GL and HS isolated and cultured hair follicles, and performed cellular experiments. GL, HL and SG raised the rabbits and conducted the animal experiments. GL, WJ and FL revised the manuscript. YZ, WJ and FL designed this work and wrote this manuscript. All authors read and approved the final manuscript.

Acknowledgements

Not applicable.

Author details

[1] College of Animal Science and Technology, Shandong Agricultural University, Tai’an 271018, P. R. China; [2] Shandong Provincial Key Laboratory of Animal Biotechnology and Disease Control and Prevention, Tai’an 271018, P. R. China; [3] Animal Husbandry and Veterinary Institute, Shandong Academy of Agricultural Sciences, Jinan 251000, P. R. China [4] Shandong Key Laboratory of Animal Disease Control and Breeding, Jinan 251000, P. R. China.

References

1. Ruben D. Choosing a Rex rabbit. Small mammal breeds. 2014.
2. Gu Z, Ren W, Huang R, Huang Y, Chen B. Study on density of rex rabbit. Chinese Journal of Rabbit Farming.1999; 4:18-21.
3. Millar SE. Molecular mechanisms regulating hair follicle development. Journal of Investigative Dermatology. 2002; 118:216–225.
4. Fuchs E. Scratching the surface of skin development. Nature. 2007;445:834-842.

5. Lin CM, Yuan Y, Chen X, Li H, Cai B, Liu Y, et al. Expression of Wnt/β–catenin signaling, stem-cell markers and proliferating cell markers in rat whisker hair follicles. Journal of Molecular Histology. 2015;46(3):233-240.
6. Demehri S, Kopan R. Notch signaling in bulge stem cells is not required for selection of hair follicle fate. Development. 2009; 136(6): 891-896.
7. Kulessa H, Turk G, Hogan BL. Inhibition of Bmp signaling affects growth and differentiation in the anagen hair follicle. Embo Journal. 2000;19(24):6664-6674.
8. Su R, Li J, Zhang W, Yin J, Zhao J, Chang Z. Expression of BMP2 in the skin and hair follicle from different stage in Inner Mongolia cashmere goat. Scientia Agricultura Sinica. 2008; 23:559-563.
9. Foitzik K, Lindner G, Mueller-Roever S, Maurer M, Botchkareva N, Botchkarev V, et al. Control of murine hair follicle regression (catagen) by TGF-beta1 in vivo. The FASEB Journal. 2000;14:752-760.
10. Greco V, Chen T, Rendl M, Schober M, Pasolli HA, Stokes N, et al. Two-step mechanism for stem cell activation during hair regeneration. Cell Stem Cell. 2009; 4(2):155–169.
11. Driskell RR, Clavel C, Rendl M, Watt FM. Hair follicle dermal papilla cells at a glance. J. Cell Sci. 2011;124:1179-1182.
12. Chi W, Wu E, Morgan BA. Dermal papilla cell number specifies hair size, shape and cycling and its reduction causes follicular decline. Development. 2013; 140:1676-1683.
13. Woo C, Eleanor W, Bruce A. Morgan permal papilla cell number specifies hair size, shape and cycling and its reduction causes follicular decline. Development and stem cells. 2013; 140: 1676-1683.
14. Yi R, Fuchs E. MicroRNAs and their roles in mammalian stem cells. J. Cell Sci. 2011; 124: 1775–1783.
15. Carrington JC, Ambros V. Role of microRNAs in plant and animal development. Science 2003; 301:336–338.
16. Xu P, Vernooy SY, Guo M, Hay BA. The Drosophila microRNA Mir-14 suppresses cell death and is required for normal fat metabolism. Curr. Biol. 2003; 13: 790–795.
17. Bartel DP. MicroRNAs: genomics, biogenesis, mechanism, and function. Cell 2004; 116:281–297.
18. Teleman AA., Maitra S, Cohen SM. Drosophila lacking microRNA miR-278 are defective in energy homeostasis. Genes Dev. 2006; 20: 417–422.
19. He L, Lim LP, Stanchina E, Xuan Z, Liang Y, Xue W, et al. A microRNA component of the p53 tumour suppressor network. Nature. 2007; 447:1130–1134.
20. Mardaryev AN, Ahmed MI, Vlahov NV, Fessing MY, Gill J H, Sharov AA, et al. Micro-RNA-31 controls hair cycle-associated changes in gene expression programs of the skin and hair follicle. FASEB Journal. 2010; 24 (10), 3869 -3881.
21. Liu Z, Xiao H, Li H, Zhao Y, Lai S, Yu X, et al. Identification of conserved and novel microRNAs in cashmere goat skin by deep sequencing. Plos One. 2012; 7(12): 50001.
22. Wang P, Hong W, Zhen J, Ren J, Li Z, Xu A. The changes of microRNA expression profles and tyrosinase related proteins in MITF knocked down melanocytes. Molecular BioSystems. 2012; 8: 2924-2931.
23. Ahmed MI, Alam M, Emelianov VU. MicroRNA214 controls skin and hair follicle development by modulating the activity of the Wnt pathway. Journal of Cell Biology. 2014; 207(4), 549-567.
24. Andl T, Murchison EP, Liu F, Zhang Y, Yunta-Gonzalez M, Tobias JW, et al. The miRNA-processing enzyme dicer is essential for the morphogenesis and maintenance of hair follicles. Current Biology. 2006;16(10), 1041–1049.
25. Shen Y, Zhang Y, Liu N, Wang H, Xie J, Gao S, et al. Let-7b promotes alpaca hair growth via transcriptional repression of TGFβRI. Gene. 2016; 577:32–36.
26. Ahmed MI, Mardaryev AN, Lewis CJ, Sharov AA, Botchkareva NV. MicroRNA-21 is an important downstream component of BMP signaling in epidermal keratinocytes. Journal of Cell Science 2011; 124(20), 3399–3404.
27. Gregory PA, Bert AG, Paterson EL, Barry SC, Tsykin A, Farshid G, et al. The miR-200 family and miR-205 regulate epithelial to mesenchymal transition by targeting ZEB1 and SIP1. Nat. Cell Biol. 2008; 10, 593–601.

28. Yi R, O\"Carroll D, Hilda AZ, Zhihong D, Fred ST, Alexander F, et al. Morphogenesis in skin is governed by discrete sets of differentially expressed microRNAs. Nat. Genet. 2006; 38, 356–362.
29. Ryan DG, Oliveira-Fernandes M, Lavker RM. MicroRNAs of the mammalian eye display distinct and overlapping tissue specificity. Mol. Vis. 2006; 12, 1175–1184.
30. Wang D, Zhang Z, O'Loughlin E, Wang L, Fan X, Lai E. et al. MicroRNA-205 controls neonatal expansion of skin stem cells by modulating the PI(3)K pathway. Nat. Cell Biol. 2013;15, 1153–1163.
31. 3 Alonso L, Fuchs E. The hair cycle. J Cell Sci 2006;119,391-3.
32. 3 Galbraith H. Fundamental hair follicle biology and fine fibre production in animals. Animal 2010;4,1490-509.
33. 3 Zhu B, Xu T, Yuan J, Guo X, Liu D. Transcriptome sequencing reveals differences between primary and secondary hair follicle derived dermal papilla cells of the Cashmere goat (Capra hircus). PloS one 2013;8, e76282.
34. Wang ZP, Zhang H, Yang H, Wang SZ, Rong EG, Pei WY, Li H, Wang N. Genome-wide association study for wool production traits in a Chinese Merino sheep population. Plos One 2014;9, e107101.
35. Liu NH, Li K, Liu J, Yu M, Cheng W, De J, Liu S, Shi Y, Zhao JS. Differential expression of genes and proteins associated with wool follicle cycling. Mol Biol Rep 2014; 41:5343-5349.
36. Meale SJ, Chaves AV, Ding S, Bush RD, McAllister TA. Effects of crude glycerin supplementation on wool production, feeding behavior, and body condition of Merino ewes. J Anim Sci 2013; 91, 878-885.
37. Wu Z, Sun L, Liu G, Liu H, Liu H, Yu Z, et al. Hair follicle development and related gene and protein expression of skins in Rex rabbits during the first 8 weeks of life. Asian-Australas J Anim Sci. 2019; 32(4):477-484.
38. Wu M, Sun Q, Guo X, Liu H. hMSCs possess the potential to differentiate intoc DP cells in vivo and in vitro. Cell Biol Int Rep. 2010; 19 (2), e00019.
39. Lim LP, Glasner ME, Yekta S, Burge CB, Bartel DP. Vertebrate microRNA genes. Science. 2003; 299, 1540.
40. Wienholds E, Plasterk RH. MicroRNA function in animal development. FEBS Lett. 2005; 579, 5911–5922.
41. Yi R., O\"Carroll D, Hilda AZ, Zhihong D, Fred ST, Alexander F, et al. Morphogenesis in skin is governed by discrete sets of differentially expressed microRNAs. Nat. Genet. 2006; 38:356–362.
42. Ryan DG, Oliveira-Fernandes M, Lavker RM. MicroRNAs of the mammalian eye display distinct and overlapping tissue specificity. Mol. Vis. 2006; 12: 1175–1184.
43. Wang D, Li Q, Feng N, Cheng G, Guan Z, Wang Y, et al. MicroRNA-205 controls neonatal expansion of skin stem cells by modulating the PI3K pathway. Nat. Cell Biol., 2013; 15:1153–1163.
44. Yu J, Peng H, Ruan Q, Fatima A, Getsios S, Lavker RM, et al. MicroRNA-205 promotes keratinocyte migration via the lipid phosphatase SHIP2. FASEB J. 2010; 24:3950–3959.
45. Lin D, Halilovic A, Yue P, Bellner L, Wang K, Wang L, et al. Inhibition of miR-205 impairs the wound-healing process in human corneal epithelial cells by targeting KIR4.1 (KCNJ10). Invest. Ophthalmol. Vis. Sci. 2013; 54:6167–6178.
46. Du T, Zamore PD. Beginning to understand microRNA function. Cell Res. 2007; 17:661–663.
47. Kollar EJ. The induction of hair follicles by embryonic dermal papillae. J. Invest. Dermatol. 1970; 55:374-378.
48. Oliver RF. The induction of hair follicle formation in the adult hooded rat by vibrissa dermal papillae. J. Embryol. Exp. Morphol. 1970; 23:219-236.
49. Jahoda CA, Horne KA, Oliver RF. Induction of hair growth by implantation of cultured dermal papilla cells. Nature1984; 311:560-562.
50. Zhang J, He X, Tong W, Johnson T, Wiedemann L, Mishina Y, et al. Bone morphogenetic protein signaling inhibits hair follicle anagen induction by restricting epithelial stem/progenitor cell activation and expansion. Stem Cells 2006; 24:2826-2839.
51. Liu G, Bai L, Li S, Liu H, Zhu Y, Sun H, et al. Isolation, culture and growth characteristics of dermal papilla cells from Rex rabbits. Tissue and Cell. 2020; 65,101348.

52. Zhang H, Wang S, Zhang T, Si H, Wang D, Yang F, et al. Epidermal growth factor promotes proliferation of dermal papilla cells via Notch signaling pathway. Biochimie 2016; 127:10-18.
53. Wang Z, Gerstein M, Snyder M. RNA-Seq: a revolutionary tool for Transcriptomics. Nature Reviews Genetics. 2009; 10(1):57-63.
54. Mortazavi A, Williams BA, McCue K, Schaeffer L. Mapping and quantifying mammalian transcriptomes by RNA-Seq. Nature Methods. 2008;5(7): 621-628.
55. Eric PN, Sarah WB, Alex B, Jennifer D, Ruth YE, Sean RE, et al. Rfam 12.0: updates to the RNA families database. Nucleic Acids Research. 2014;43: D130-137.
56. Kozomara A, Griffiths-Jones S. miRBase: annotating high confidence microRNAs using deep sequencing data. NAR. 2014;42: D68-D73.
57. Friedlander MR, Chen W, Adamidic C, Maaskoia J, Einspanier R, Knespel S, et al. Discovering microRNAs from deep sequencing data using miRDeep. Nature Biotechnology 2008;26:407-415.
58. Peter AC, Yavuz A, Heleneb HT, Erno V, Rolf H, Renée X, Judith M, et al. Deep sequencing-based expression analysis shows major advances in robustness, resolution and inter-lab portability over five microarray platforms. Nucleic Acids Res. 2008;36(21): e141.
59. Jiang H, Wong WH. Statistical inferences for isoform expression in RNASeq. Bioinformatics 2009;25:1026-1032.
60. Yang YH, Dudoit S, Luu P, Lin DM, Peng V, Ngai J. Normalization for cDNA microarray data: a robust composite method addressing single and multiple slide systematic variation. Nucleic Acids Res. 2002;30: e15.
61. Wang L, Feng Z, Wang X, Wang X, Zhang X. DEGseq: an R package for identifying differentially expressed genes from RNA-seq data. Bioinformatics. 2010;26(1):136-138.
62. John B, Enright AJ, Aravin AA, Tuschl T, Sander C, Marks DS. Human MicroRNA targets. Plos. Biology. 2005;3(7), e264.
63. Kanehisa M, Araki M, Goto S, Hattori M, Hirakawa M, Itoh M, et al. KEGG for linking genomes to life and the environment. Nucleic Acids Res. 2008;36: D480-484.
64. Ouji Y, Yoshikawa M, Moriya K, Ishizaka S. Effects of Wnt-10b on hair shaft growth in hair follicle cultures. Biochem. Biophys. Res. Commun. 2007;359:516–522.
65. LiLivak KJ, Schmittgen TD. Analysis of relative gene expression data using real-time quantitative PCR and the $2^{-\Delta\Delta CT}$ method. Methods. 2001; 25: 402–408.

Tables

Table 1. Effects of ocu-miR-205 on proliferation, cell cycle and apoptosis of dermal papilla cells (DPCs; %)

Items	Group				R-MSE	*P*-value
	Control	HBAD-GFP	HBAD-ocu-miR-205-GFP	HBAD-ocu-miR-205-5p-sponge-GFP		
Proliferation of dermal papilla cells						
Optical density (OD) value	0.56±0.01^{b}	0.55±0.01^{b}	0.61±0.01^{a}	0.34±0.01^{c}	0.0356	<0.0001
Cell cycle of dermal papilla cells						
Resting state/first gap (G0/G1)	87.79±1.00^{a}	84.68±1.01^{b}	77.71±0.88^{c}	85.57±1.03^{ab}	2.7795	<0.0001
Synthesis (S)	7.15±0.85^{b}	9.48±0.95^{b}	14.73±0.62^{a}	8.97±0.68^{b}	2.2232	<0.0001
Second gap/mitosis (G2/M)	5.07±0.24^{b}	5.37±0.49^{b}	7.56±0.37^{a}	5.46±0.35^{b}	1.0523	0.0002
Apoptosis of dermal papilla cells						
Early apoptotic ratio (Q4)	33.95±0.40^{b}	32.86±1.04^{b}	36.71±0.67^{a}	29.16±0.47^{c}	1.9470	<0.0001
Later apoptotic ratio (Q2)	33.46± 0.57^{b}	32.15±1.33^{b}	36.11±0.73^{a}	31.40±0.57^{b}	2.4323	0.0032
Total apoptosis ratio (Q4+Q2)	67.41±0.51^{b}	65.01±1.50^{b}	72.83±1.14^{a}	60.56±0.47 ^{b}	2.8310	<0.0001

Note: Data shown are mean values ± s. d., and n = 8 per group. In the same row, values with same letter superscripts mean no significant difference (P>0.05), with different letter superscripts mean significant difference (P<0.05).

Table 2. Effects of ocu-miR-205 on gene expression of signal pathway of dermal papilla cells (DPCs)

Gene	Group				R-MSE	*P*-value
	Control	HBAD-GFP	HBAD-ocu-miR-205-GFP	HBAD-ocu-miR-205-5p-sponge-GFP		
PI3K/Akt signal pathway						
Inppl1	1.00±0.09^{b}	1.02±0.04^{b}	0.80±0.07^{b}	1.68±0.12^{a}	0.2353	<0.0001
Inpp4b	1.00± 0.09	0.97±0.16	0.92±0.08	1.21±0.16	0.3598	0.3966
Frk	1.00±0.34^{b}	0.90±0.07^{b}	0.50±0.13^{c}	2.63±0.47^{a}	0.8442	0.0001
Phlda3	1.00± 0.04^{b}	0.89±0.06^{b}	0.69±0.05^{c}	1.18±0.05^{a}	0.1491	<0.0001
Wnt signal pathway						
Wnt10b	1.00±0.11^{b}	0.95±0.09^{b}	0.38±0.11^{c}	2.24±0.17^{a}	0.3519	<0.0001
CTNNB1	1.00±0.09^{b}	1.50±0.13^{b}	1.48±0.19^{b}	3.16±0.27^{a}	0.5186	<0.0001
GSK-3β	1.00± 0.14^{b}	0.97±0.05^{b}	2.66±0.68^{a}	3.22±0.71^{a}	1.4118	0.0050
DKK1	1.00±0.09^{c}	2.90±0.13^{b}	6.09±0.84^{a}	0.84±0.07^{c}	1.2141	<0.0001
Notch signal pathway						
Notch1	1.00±0.08^{b}	0.96±0.07^{b}	0.39±0.02^{c}	1.19±0.03^{a}	0.1604	<0.0001
Jagged1	1.00±0.07^{ab}	0.81±0.13^{bc}	0.60±0.10^{c}	1.12±0.07^{a}	0.2679	0.0032
Hes1	1.00±0.12^{b}	1.19±0.16^{b}	0.90±0.05^{b}	2.40±0.33^{a}	0.5475	<0.0001
Hes5	1.00± 0.16^{b}	1.04±0.06^{b}	0.18±0.04^{c}	1.38±0.04^{a}	0.2477	<0.0001
BMP signal pathway						
BMP2	1.00±0.15^{b}	0.51±0.05^{bc}	1.69±0.34^{a}	0.41±0.05^{c}	0.5408	0.0002
BMP4	1.00± 0.20^{ab}	1.11±0.18^{ab}	1.34±0.08^{a}	0.63±0.13^{b}	0.4405	0.0254
TGF-β1	1.00±0.05^{ab}	0.89±0.18^{b}	1.33±0.13^{a}	0.71±0.07^{b}	0.3304	0.0071

Note: Data shown are mean values ± s. d., and n = 8 per group. In the same row, values with no letter superscripts or same letter superscripts mean no significant difference (*P*>0.05), with different letter superscripts mean significant difference(*P*<0.05).

Table 3. Effects of ocu-miR-205 on gene expression of signal pathway of Rex rabbits skin

Gene	Group				R-MSE	*P*-value
	Control	HBAD-GFP	HBAD-ocu-miR-205-GFP	HBAD-ocu-miR-205-5p-sponge-GFP		
PI3K/Akt signal pathway						
Inppl1	1.00±0.09^{b}	0.99±0.07^{b}	0.54±0.03^{c}	2.30±0.15^{a}	0.2731	<0.0001
Inpp4b	1.00± 0.15^{ab}	0.89± 0.07^{a}	0.09±0.01^{b}	1.05±0.02^{a}	0.2348	<0.0001
Frk	1.00±0.26^{a}	1.16±0.05^{b}	0.31±0.02^{c}	1.94±0.20^{a}	0.4666	<0.0001
Phlda3	1.00± 0.11^{b}	1.18± 0.11^{a}	0.27±0.03^{b}	1.18±0.11^{a}	0.2500	<0.0001
Wnt signal pathway						
Wnt10b	1.00±0.14^{b}	0.86±0.04^{bc}	0.74±0.04^{c}	1.26±0.09^{a}	0.2406	0.0011
CTNNB1	1.00±0.07^{b}	0.98±0.05^{b}	0.75±0.04^{c}	1.30±0.08^{a}	0.1789	<0.0001
GSK-3β	1.00± 0.06^{ba}	1.04±0.07^{b}	0.85±0.04^{b}	1.10±0.05^{a}	0.1496	0.0198
DKK1	1.00±0.36^{a}	0.91±0.10^{a}	1.28±0.10^{a}	0.18±0.07^{b}	0.5625	0.0041
Notch signal pathway						
Notch1	1.00±0.18^{b}	0.83±0.05^{bc}	0.54±0.05^{c}	1.95±0.22^{a}	0.4131	<0.0001
Jagged1	1.00±0.13^{a}	1.02±0.05 ^{a}	0.36±0.03^{c}	1.34±0.22 ^{a}	0.3670	0.0001
Hes1	1.00±0.09^{b}	1.03±0.06^{b}	0.80±0.03^{b}	1.49±0.18^{a}	0.3042	0.0009
Hes5	1.00± 0.13 ^{b}	1.00±0.05^{b}	0.36±0.03^{c}	1.43±0.20^{a}	0.3435	<0.0001
BMP signal pathway						
BMP2	1.00±0.15^{b}	1.02±0.07^{b}	1.39±0.08^{a}	0.64±0.10^{c}	0.3051	0.0005
BMP4	1.00± 0.15^{b}	0.87±0.04^{b}	1.58±0.14^{a}	0.73±0.05^{b}	0.3081	<0.0001
TGF-β1	1.00±0.12 ^{ab}	0.88±0.05 ^{bc}	1.15±0.06^{a}	0.67±0.05^{b}	0.2222	0.0014

Note: Data shown are mean values ± s. d., and n = 8 per group. In the same row, values with same letter superscripts mean no significant difference (P>0.05), with different letter superscripts mean significant difference (P<0.05).

Table 4. Effects of ocu-miR-205 on hair follicle density of Rex rabbits (Count/mm^2)

Items	Group				R-MSE	*P*-value
	Control	HBAD-GFP	HBAD-ocu-miR-205-GFP	HBAD-ocu-miR-205-5p-sponge-GFP		
Transfection for 7 days						
Hair follicle density	125.57±9.63^{bc}	144.25±11.47^{ba}	105.02±5.89^{c}	163.94±16.68^{a}	32.7817	0.0085
Primary hair follicle density	10.08±0.85	9.31±0.85	7.80±0.63	9.79±0.77	2.2046	0.1902
Secondary hair follicle density	115.49±9.48^{bc}	134.93±12.01^{ba}	97.22±5.68^{c}	154.15±16.65^{a}	32.9728	0.0113
Secondary/Primary (S/P) ratio	11.92±1.17	16.02±2.67	12.92±1.06	16.38±2.04	5.2469	0.2536
Transfection for 14 days						
Hair follicle density	130.54±12.22^{b}	136.62±8.51^{b}	119.30±7.24^{b}	203.34±14.79^{a}	31.4005	<0.0001
Primary hair follicle density	10.86±0.54	9.96±0.50	11.92±0.74	10.11±0.70	1.7739	0.1307
Secondary hair follicle density	119.68±12.03^{b}	126.66±8.28^{b}	107.37±7.10^{b}	213.32±14.62^{a}	30.9035	0.0001
Secondary/Primary (S/P) ratio	11.08±0.96 ^{b}	12.82±0.82 ^{b}	9.20±0.78 ^{b}	21.62±1.94 ^{a}	3.4505	<0.0001
Transfection for 21 days						
Hair follicle density	145.43±13.71^{b}	139.58±16.53^{b}	126.38±9.30^{b}	208.69±21.42^{a}	44.8651	0.0049
Primary hair follicle density	14.30±1.19	12.65±0.80	12.92±0.51	15.29±1.28	2.8084	0.2244
Secondary hair follicle density	131.13±13.21^{b}	126.94±16.57^{b}	113.46±9.27^{b}	193.40±21.31^{a}	44.4697	0.0060
Secondary/Primary (S/P) ratio	9.45±0.91	10.28±1.40	8.86±0.75	13.28±1.85	3.6808	0.1018

Note: Data shown are mean values ± s. d., and n = 8 per group. In the same row, values with no letter superscripts or same letter superscripts mean no significant difference (P>0.05), with different letter superscripts mean significant difference (P<0.05).

Additional File Legends

Additional file 1:

Supplementary Figure 1. Skin crosscutting HE staining of Rex rabbits with different hair density（100 magnification）(a) Low hair density (b) High hair density

Supplementary Table 1. Statistics of hair follicle numbers of Rex rabbits with different hair density

Note: Data shown are mean values ± s. d., and n =3 per group. In the same row, values with with different letter superscripts mean significant difference(P<0.05).

Additional file 2:

Supplementary Table 2. RNA quality of six DPC samples Supplementary Figure 2. RNA quality (a) Agarose electrophoresis of RNA in DPCs; (b) Quality test results of total RNA by Agilent 2100

Additional file 3:

Supplementary Table 3. Statistics of sequence data of each samples

Additional file 4:

Supplementary Figure 3. Length distribution map of Small RNA

The X-axis is the length of small RNA, and the Y-axis is the corresponding number of small RNA

Additional file 5:

Supplementary Table 4. Alignment clean tag in genome

Additional file 6:

Supplementary Figure 4. Statistical distribution map of small RNA types

In order to make each unique small RNA have a unique annotation, the annotation statistics of small RNA traverse the annotation according to the priority order of microRNA > piRNA > snoRNA > Rfam > other sRNA.

Additional file 7:

Supplementary Figure 5. The quantity distribution maps of clean tag base in each sample

The X-axis is the position of the base in read, and the Y-axis represents the proportion of the base.

Additional file 8:

Supplementary Figure 6. The quality distribution maps of the clean tag base in each sample

The X-axis is the position of base in read, and the Y-axis represents the base mass value.

Additional file 9:

Supplementary Table 5. LD-vs-HD_DEGseq.diffexpfilter

Additional file 10:

Supplementary Table 6. Primer sequence information in experiment

Figures

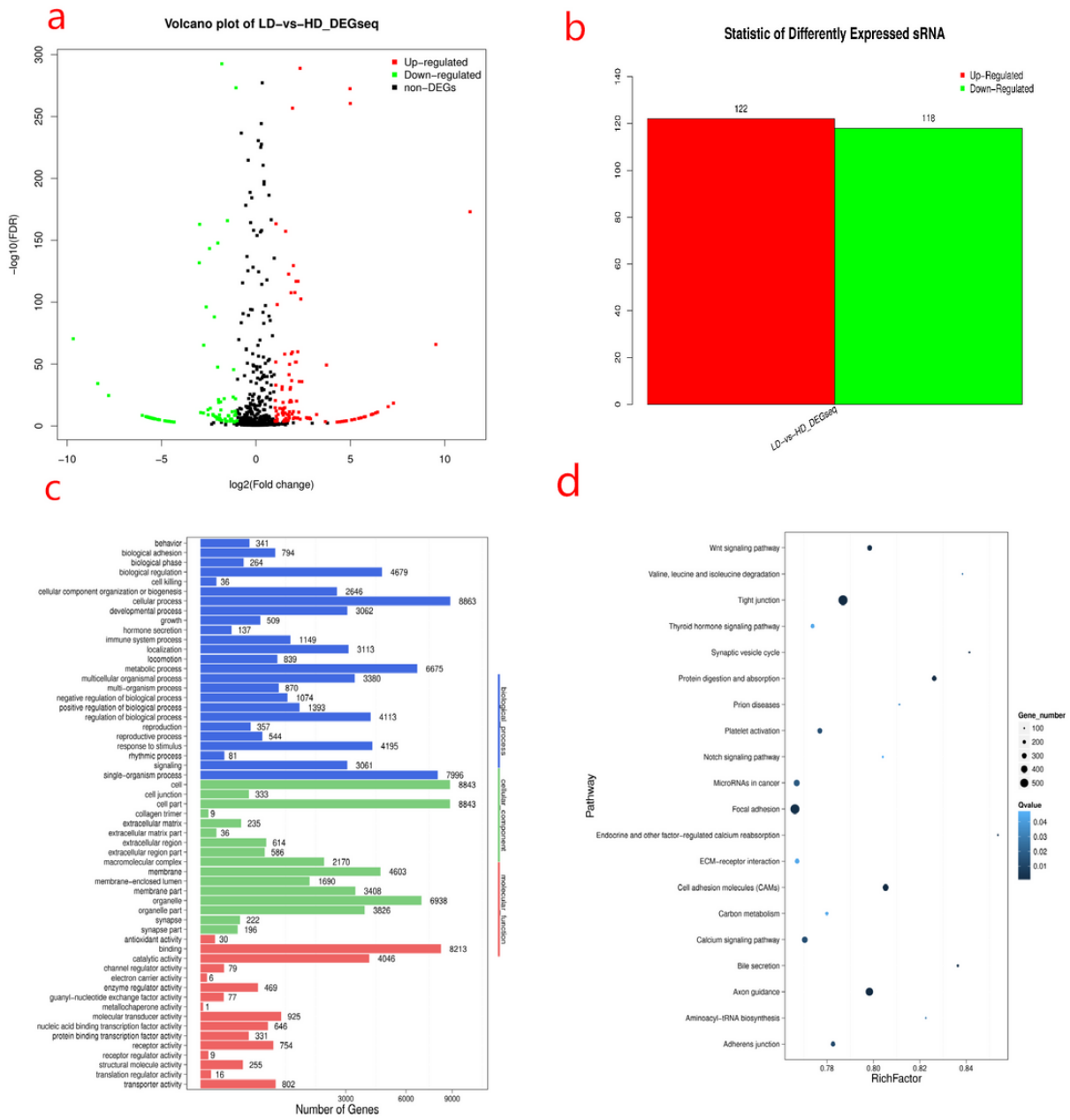

Figure 1

Differentially expressed miRNAs (a) Differential miRNAs volcanic map; (b) Significantly differential expressed miRNAs; (c) GO functional classification of differential miRNA target genes; (d) Pathway enrichment statistical scatter plot

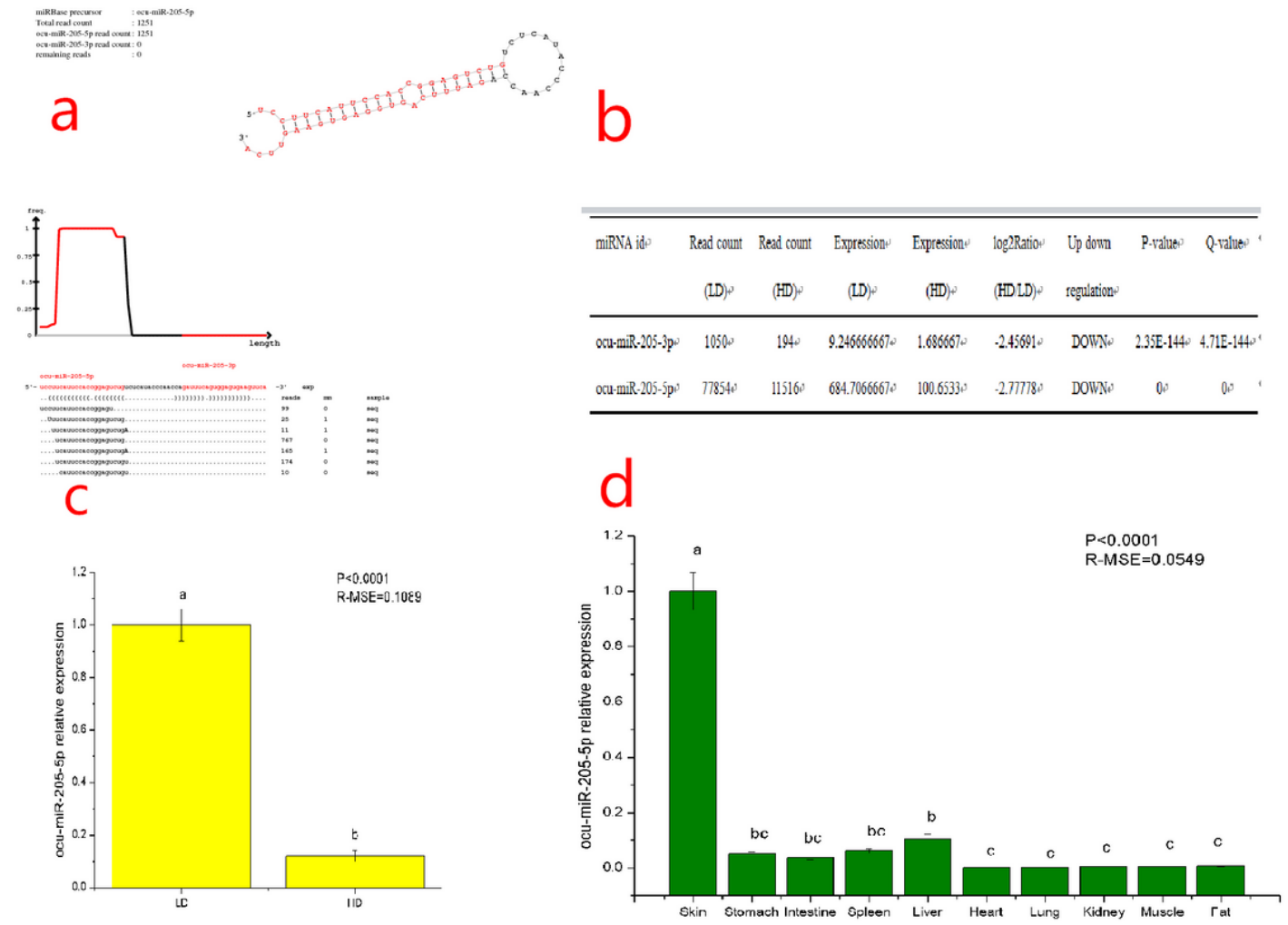

miRNA id	Read count (LD)	Read count (HD)	Expression (LD)	Expression (HD)	log2Ratio (HD/LD)	Up down regulation	P-value	Q-value
ocu-miR-205-3p	1050	194	9.246666667	1.686667	-2.45691	DOWN	2.35E-144	4.71E-144
ocu-miR-205-5p	77854	11516	684.7066667	100.6533	-2.77778	DOWN	0	0

Figure 2

Expression of ocu-miR-205-5p (a) Structure of ocu-miR-205; (b) Expression of ocu-miR-205 in dermal papilla cells of rabbits with different density detected by high-throughput sequencing; (c) Real-time PCR analysis of ocu-miR-205-5p expression in dermal papilla cells with different hair density. Mean values ± s.d., n =3, a,b mean P< 0.05. (d) Real-time PCR analysis of ocu-miR-205-5p expression in different tissues of Rex rabbits, Mean values ± s.d., n=8, a,b mean P< 0.05. Rex rabbits were 30 days old, four for male, four for female.

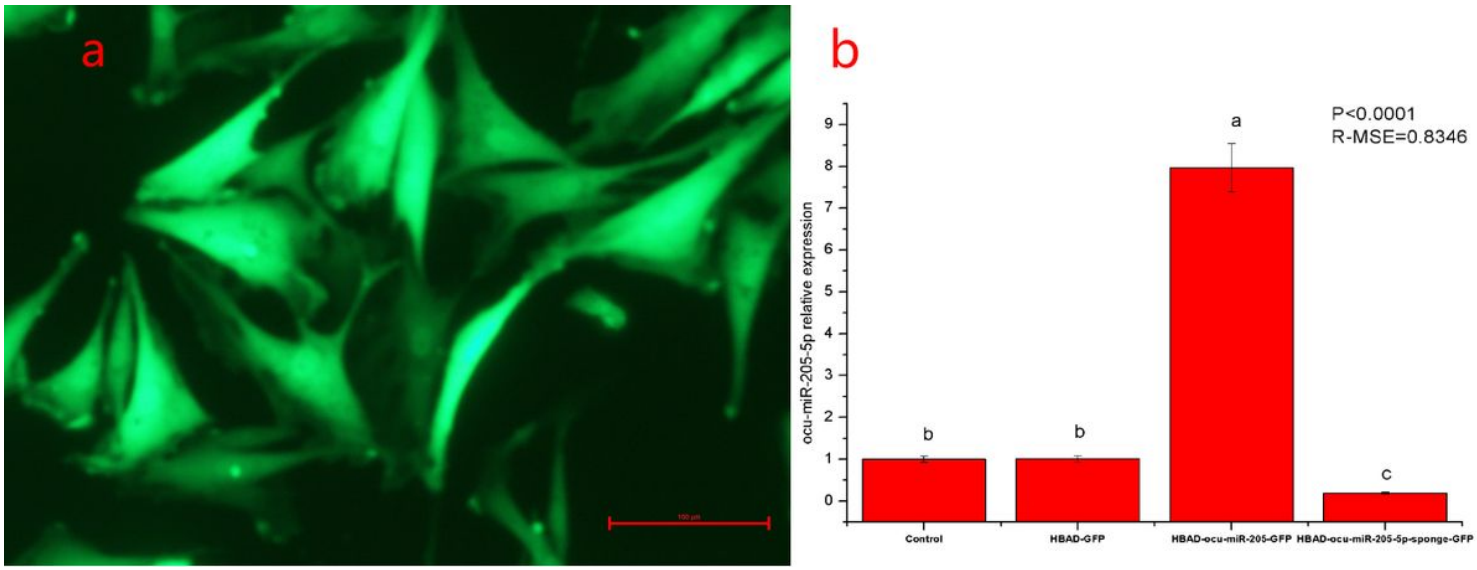

Figure 3

Effects of adenovirus transfection on DPCs (a) Transfection 24h, fluorescence microscope (200 magnification); (b) Expression of ocu-miR-205-5p in dermal papilla cells after transfection 48 h detected by quantitative fluorescence quantification, Mean values ± s.d., a,b mean P< 0.05, n=8.

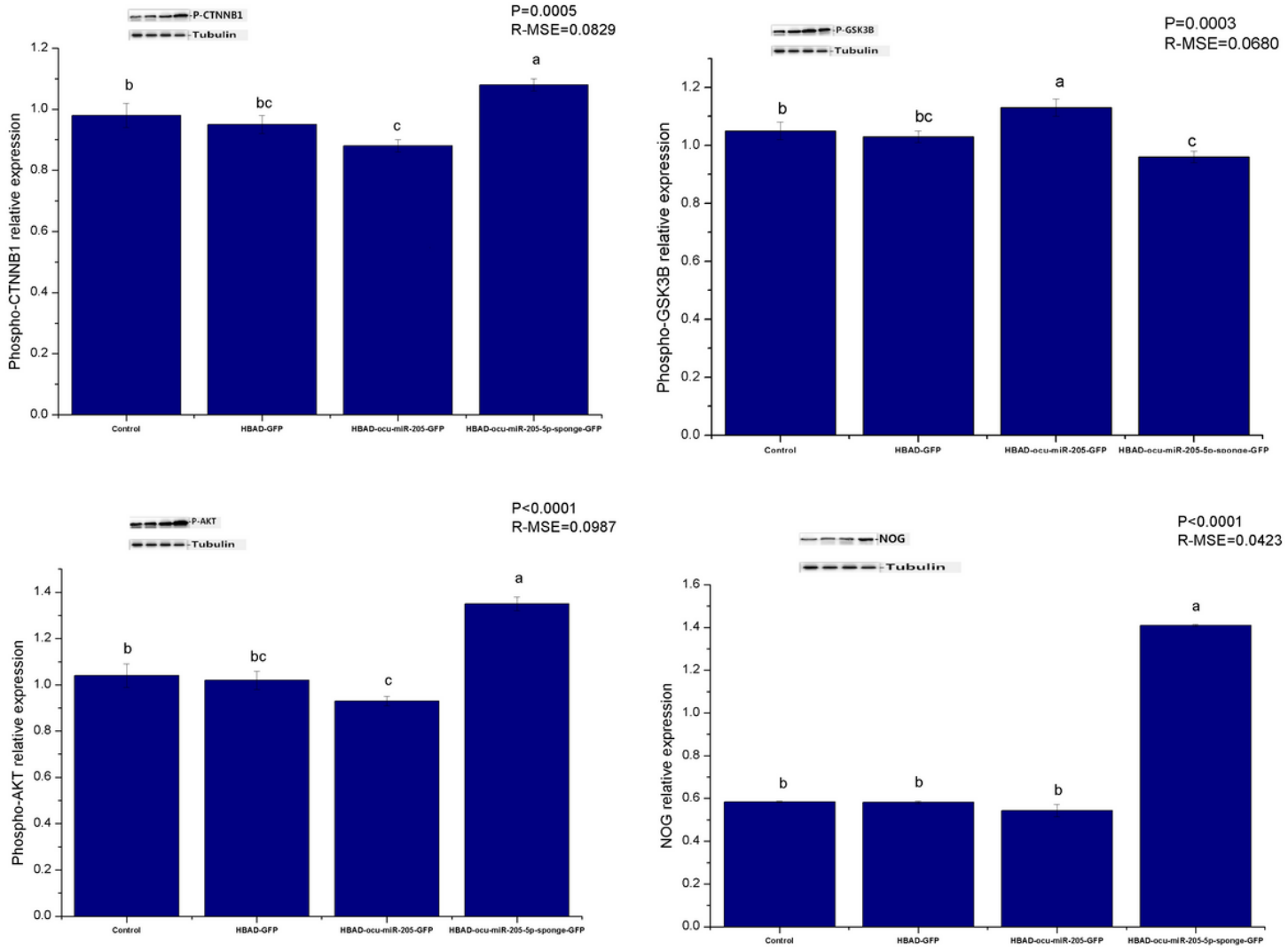

Figure 4

Effects of ocu-miR-205 on expression of hair follicle-related proteins of DPCs Mean values ±s.d., and n = 8 per group. In the same graph, values with same letter superscripts mean no significant difference (P>0.05), with different letter superscripts mean significant difference (P<0.05).

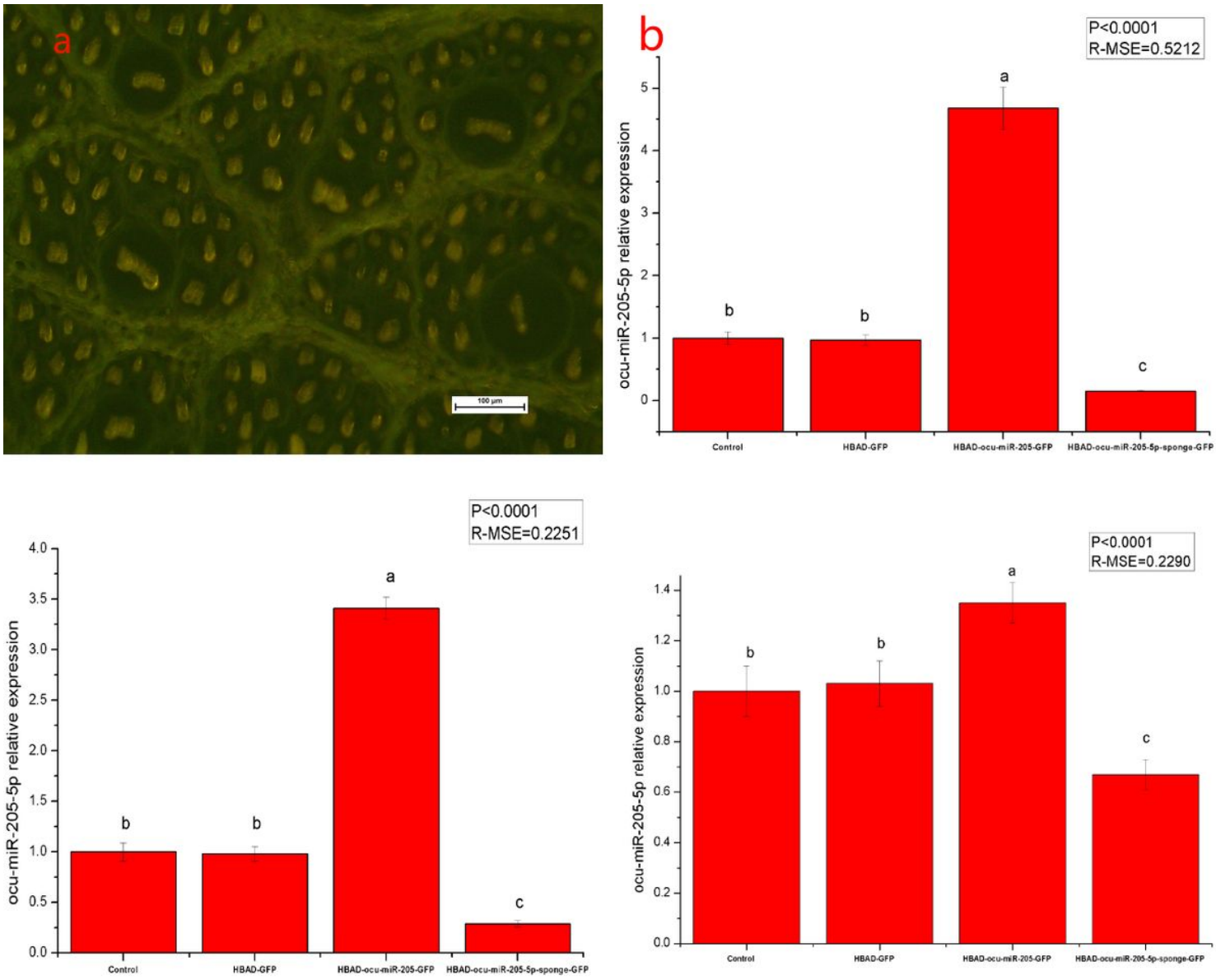

Figure 5

Effects of adenovirus transfection on skin follicles of Rex rabbits (a) Frozen slice crosscutting of Rex rabbits skin (200 magnification); (b) Expression of ocu-miR-205-5p in dermal papilla cells after transfection 7d, 14d, 21d detected by quantitative fluorescence quantification, Mean values ±s.d., a,b mean P< 0.05, n=8.

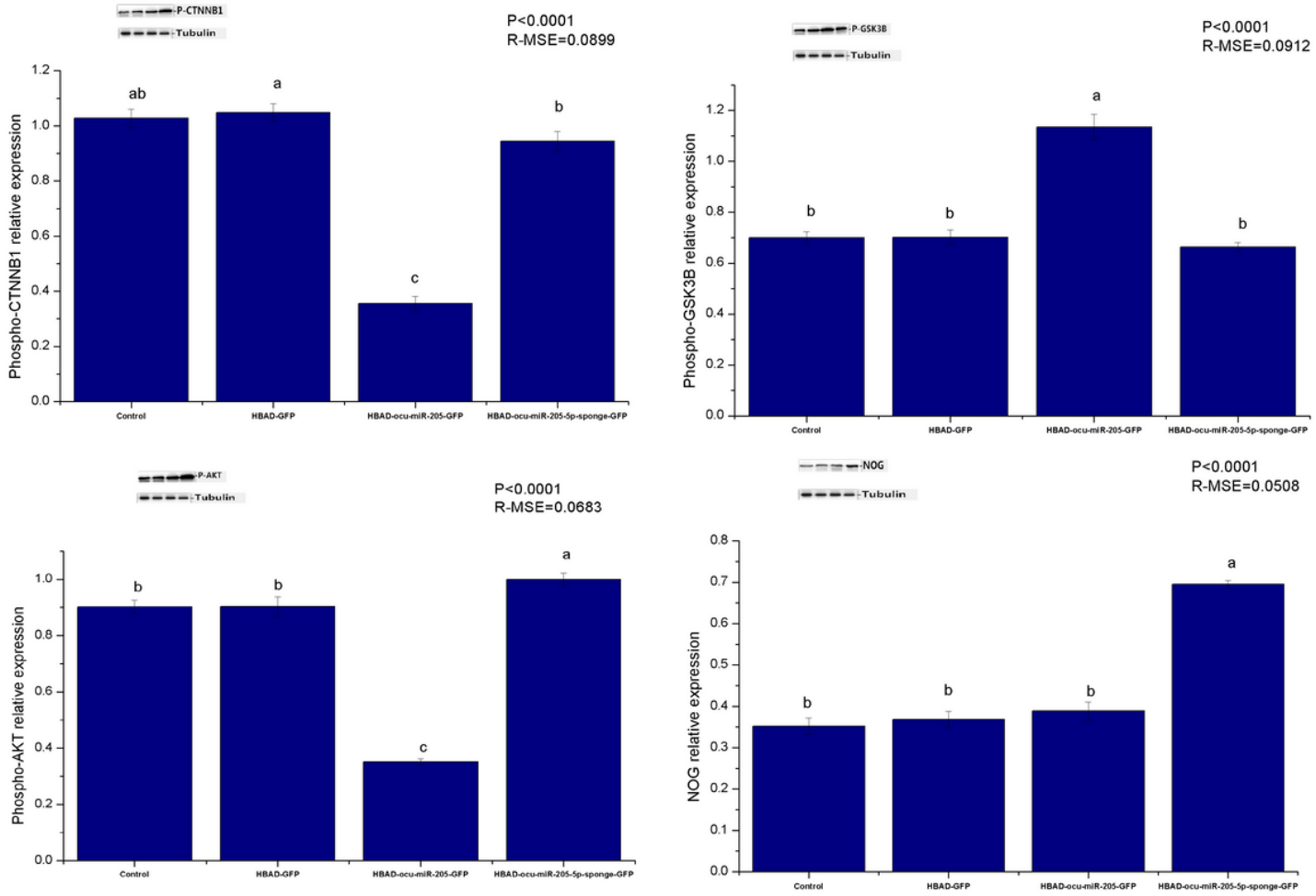

Figure 6

Effects of ocu-miR-205 on expression of hair follicle-related proteins of Rex rabbits skin Mean values ± s.d., and n = 8 per group. In the same graph, values with same letter superscripts mean no significant difference (P>0.05), with different letter superscripts mean significant difference (P<0.05).

Supplementary Files

This is a list of supplementary files associated with this preprint. Click to download.

- SupplementaryFigure5LD3.png
- SupplementaryFigure4LD2.png
- SupplementaryFigure5LD1.png
- SupplementaryFigure5HD3.png
- SupplementaryFigure4LD3.png
- SupplementaryFigure5HD2.png
- SupplementaryFigure4HD3.png
- SupplementaryFigure5HD1.png
- SupplementaryFigure1b.jpg
- SupplementaryFigure4HD2.png

- SupplementaryFigure4LD1.png
- SupplementaryFigure6LD3.png
- SupplementaryFigure6LD2.png
- SupplementaryFigure6LD1.png
- SupplementaryFigure6HD2.png
- SupplementaryFigure6HD3.png
- SupplementaryFigure6HD1.png
- SupplementaryFigure4HD1.png
- SupplementaryFigure2bLD3.png
- SupplementaryTable6.docx
- SupplementaryTable5.LDvsHDDEGseq.diffexpfilter.xls
- SupplementaryTable14.docx
- SupplementaryFigure2a.png
- ARRIVEchecklist.docx
- SupplementaryFigure3HD2.png
- SupplementaryFigure2bLD2.png
- SupplementaryFigure2bHD3.png
- SupplementaryFigure2bHD1.png
- SupplementaryFigure2bLD1.png
- SupplementaryFigure2bHD2.png
- SupplementaryFigure3LD3.png
- SupplementaryFigure3LD2.png
- SupplementaryFigure3HD1.png
- SupplementaryFigure3LD1.png
- SupplementaryFigure1a.jpg
- SupplementaryFigure3HD3.png
- SupplementaryFigure5LD2.png